Hindawi
International Journal of Aerospace Engineering
Volume 2019, Article ID 3742123, 8 pages
https://doi.org/10.1155/2019/3742123

Research Article

Conceptual Design of Spacesuit Hard Hip Joint

Wang Zhen-wei, Chen Peng, and Lin Dan-lan

School of Aeronautics and Astronautics, University of Electronic Science and Technology of China, Chengdu 611731, China

Correspondence should be addressed to Wang Zhen-wei; wangjanvey@163.com

Received 22 February 2019; Revised 2 July 2019; Accepted 31 August 2019; Published 17 September 2019

Academic Editor: Marco Pizzarelli

Spacesuit hip joint plays an important role on astronaut activities, such as planetary walking and surveying. This paper proposes a conceptual design of hard hip joint in consideration of the coupling effect of spacesuit hip joint and astronaut thigh. Firstly, lower extremity activities are introduced to illustrate the mobility of hard hip joint, such as walking, kneeing, and abduction. A conceptual design of hard hip joint is explained in detail, including geometric structure, components, design parameters, and mechanism models. Secondly, a 3-linkage coupling mechanism model is built up by synthesizing that conceptual design of hard hip joint. An equiangular dual-perpendicular representation method is brought out to parameterize that mechanism model of hard hip joint. Particularly, four geometric constraints are, respectively, given out to avoid impact between the hip joint and the thigh and to ensure the continuity of thigh motion. Finally, motion equations of hip joint parts are established by using coordinate transformation and vector representation. A case study is conducted to verify the correctness of the proposed representation method and that coupling mechanism model.

1. Introduction

Hip joint is an important component in spacesuit, which enables mobility of astronauts wearing pressurized spacesuits to complete missions, including walking and surveying. Hip joint is briefly classified into soft hip joint and hard hip joint. Generally, hard hip joint is made of some rigid materials, such as aluminum alloy and stiffness composite. Soft hip joint is made of soft materials, such as nylon and fabric. General spacesuit is pressurized with gas to a certain pressure level making it stiff in the vacuum of space [1]. For soft hip joint, the stiffen spacesuit greatly increase unnecessary energy expenditure and impeded mobility. Additional factors also include change in suit column and fabric stiffness as the joints bend [2]. Relatively, hard hip joint can avoid above problems because deformation of rigid material caused by pressurized gas is very little. The major advantage of hard joint is that torque moment derived by bearing friction is less than other kinds of hip joint. Therefore, hard hip joint has been widely applied to some spacesuits, such as the *Z* series spacesuit [3] and Mark III spacesuit [4]. On the other hand, the primary problem of hard joint is that the placement of bearings causes programming and potentially unnatural movement and stances. Presently, it is one of technical bottlenecks.

Spacesuit field involves many topics widely, such as mobility and agility [5], human-suit interaction [6], astronaut injury estimation [7], joint torque testing [8], human movements [9, 10], and gait simulation [11, 12]. Among those topics, hip joint mobility is one of the basic research focuses. Around joint mobility, many kinds of spacesuit joint had been developed, including flat-pattern joint, bellow-type joint, and rotation-bearing joint. Now, there are many research achievements in motion analysis and test [13, 14], computational methods [15, 16], human factors [17, 18], and joint development [19, 20]. As far as joint design is concerned, there is relatively less research on the improvement of hard joint design for many years. With the development of planetary explorations, a new spacesuit design is becoming more important, such as Mars exploration and lunar landing.

Spacesuit is different from other classical spacecraft, which is characterized as the human-suit interactive spacecraft. As for spacesuit hip joint, there exists a strong coupling effect between hip joint and astronaut thigh. The coupling effect is embodied by impact, rubbing, etc. Therefore, the conceptual design of hip joint should pay attention to above coupling effect. To solve above problem, this paper brings forward an equiangular dual-perpendicular representation method and two related geometric constraints. Moreover, a 3-linkage coupling mechanism model is constructed based on a conceptual model of the hip joint. That coupling mechanism model is helpful for parametric design and motion analysis. To ensure the motion continuity of the joint and thigh, two additional geometric constraints are brought out and discussed in detail. Furthermore, motion equations of hip joint part are established using coordinate transformation and vector representation. Finally, a case study is conducted to verify the correctness of the proposed representation method and coupling mechanism model of the hip joint.

2. Conceptual Design of Hard Hip Joint

2.1. Conceptual Model of Hip Joint. Four basic lower extremity activities of designed spacesuit are illustrated in Figure 1, including standing, walking, kneeing, and abduction. Those activities require the hip joint to be mobile and flexible. Although four activities appear different, they can be generalized as hip joint motion based on kinematics. Namely, every activity corresponds to specific rotation of the hip joint, but their rotational angles are different from each other. Also, Figure 1 shows some joints and components in designed spacesuit. This paper only discusses the hip joint, where it is made of aluminum alloy and designed to connect the waist part with the thigh part. When a suited astronaut moves the thigh, related hip joint will be driven to move synchronously. Thus, low extremity activities can be performed. Around the hip joint, the following sections will discuss its components, geometric structure, and design parameters.

Conceptual models of the hip joint and its components are constructed, as shown in Figure 2. From a view of mechanism design, the hip joint can be regarded as a rigid assembly with 3 degrees-of-freedom, where the hip joint consists of briefs part, right hip joint, left hip joint, and rotation bearings. Bearings are not displayed due to no effect on conceptual design. The structure of left and right hip joint is designed to be the same. It is composed of two parts—upper part and lower part. Both parts are connected together by a rotation bearing. Similarly, briefs part is, respectively, connected with two hip joint parts by rotation bearings. Due to rotation bearings, low part and high part can rotate independently. In other words, thigh motion can be decomposed into relative rotations of upper and lower parts. That is the basic thought for the conceptual design of the hip joint.

2.2. Geometric Structure of Hip Joint Part. To reduce manufacturing cost, a similar geometric structure is used to design upper part and lower part, as shown in Figure 3. As a whole, it is a shell body with uniform thickness of 5 mm. With neglect of thickness, the geometric structure is formed by two tangent circles with inclined angle a_i and one ruled surface sweeping from upper circle to lower circle. Where P is the tangent point of two circles, O_l and O_u are the corresponding center point of lower circle and upper circle. Through those three points, a central plane is constructed to parameterize joint part. Moreover, a local coordinate frame $x_i y_i z_i$ is also established to express the geometric shape of joint part. In a central plane, the geometric structure can be represented by parameters r_i, r_{i+1}, and a_i completely, where r_i and r_{i+1} are the radius of upper circle and lower circle, respectively. Subscript i is the index of joint part, i.e., $i = 1$ or 2, and number 1 stands for upper part. These parameters are determined according to design requirements.

Due to large stiffness, hip joint part is treated as a rigid body theoretically. Thus, the geometric structure can be synthesized to be one link from point O_l to point O_u based on the mechanism theory. Moreover, a rotation joint is placed at point O_l to connect other joint part. Generally, link is not required to be perpendicular to two circles. On the contrary, rotation joint must be vertical to lower circle to ensure relative rotation of hip joint part. As a result, upper and lower parts can be, respectively, represented as links and parameterized by sets $\{r_1, r_2, \text{and } a_1\}$ and $\{r_2, r_3, \text{and } a_2\}$. Considering rigidity of human bone, we also simplify thigh as one link with a spherical joint. Although this simplification causes error, it is helpful for analytical solution of joint motion. Above all, joint parts and thigh can be regarded as link under a condition of enough stiffness.

2.3. Coupling Mechanism of Hip Joint Assembly. By combining the thigh with the hip joint, a hip joint assembly is constructed, as shown in Figure 4(a). It consists of astronaut torso, thigh, briefs part, and hip joint. Generally, spacesuit mounted on astronaut should be by internal textile belt. A fixed belt in the waist joint is used to restrict lateral location. Thus, briefs part location is deterministic related to astronaut. The location limit is not our research objective. We do not discuss it anymore.

By assembling above links, a 3-linkage coupling mechanism model of hip joint assembly can be built up, as shown in Figure 4(b). It consists of three links, one cylindrical joint, two rotation joints, and ground base, where links 1, 2, and 3 correspond to upper part, lower part, and thigh, respectively. Astronaut torso is modeled as ground base. Link 1 connects with ground base by rotation joint 1 and with link 2 by rotation joint 2. Relative rotation of link 1 and link 2 can be measured by angles θ_1 and θ_2. Particularly, link 3 is connected with link 2 by cylindrical joint and with ground base by spherical joint. In order to ensure motion consistency between human thigh and hip joint, link 3 needs to be located at original point o. In other words, spherical joint and rotational joint 1 are coincident to original point o. All links are measured and expressed in reference coordinate frame xyz. More details about coordinate frame xyz will be discussed in Section 3.2.

3. Parameter Calculation of Hip Joint

3.1. Parameterization of Hip Joint. Generally, there are many requirements on spacesuit, such as motion, safety, strength, and weight. This paper is mainly aimed at impacting and motioning continuity. To solve above two problems, an equiangular dual-perpendicular method is firstly brought out to parameterize a conceptual model of hard hip joint, as illustrated in Figure 5, where upper part and lower part are

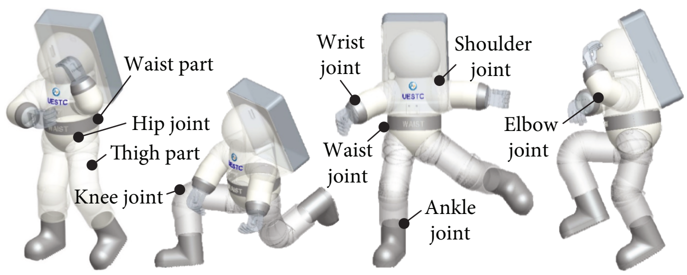

Figure 1: Four basic lower extremity activities of designed spacesuit.

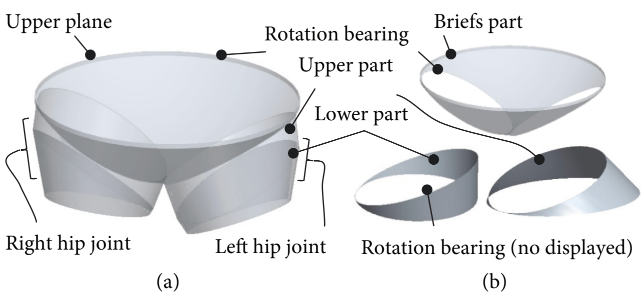

Figure 2: Conceptual models of the (a) hip joint and (b) its components.

aligned with their central planes. Initial angles of two joint parts equal to zero, $\theta_1 = \theta_2 = 0$, where links 1, 2, and 3 are represented by segment lines *JC*, *CE*, and *JE*, respectively. It can be seen that lengths of segment lines *PJ*, *PC*, and *PE* are equal to radiuses r_1, r_2, and r_3, respectively. Next, we will introduce four geometric constraints in order to avoid impact and ensure motion continuity.

To avoid impact between the hip joint and the thigh, two geometric constraints must be satisfied. The first constraint is that both segment lines *JE* and *JC* are, respectively, perpendicular to segment lines *PE* and *PC*. The second constraint is that segment line *PC* is a diagonal line of angle $\angle JPE$. It can be concluded that above constraints enable segment line *JE* to be perpendicular to the lower circle of lower part all the time. In other words, impact will not happen between the hip joint and the thigh. Moreover, above two constraints cause inclined angle a_1 to be equal to inclined angle a_2, $a_1 = a_2$.

In order to ensure continuous motion of the thigh, two geometric constraints are proposed in addition. The first constraint is that segment line *CE* and *CD* is symmetric about segment line *CJ*. The second constraint is that point *D* must lie in coordinate axis *z*. Under condition of above two constraints, motion continuity means that segment line *JE* can rotate around point *J* freely. Namely, segment line *JE* is a fixed point rotation. According to kinematics, rotation around fixed point *J* can be discomposed into a planar rotation around point *J* and a rotation around coordinate axis *z*. Obviously, the latter rotation is continuous. So, main difficulty is how to realize the continuity of planar rotation. As mentioned above, two additional constraints enable segment line *JE* to rotate along planar arc l_r. As a result, motion continuity is realizable according to above geometric constraint.

Above all, those problems can be solved by introducing four geometric constraints, including two perpendicular constraints, one symmetric constraint and one coincident constraint.

Based on above four constraints, structure parameters of hip joint and briefs part can be obtained. Next, we derive the structure parameters of hip joint. In Figure 5, parameters r_1 are determined by design requirement and parameter α_d is given as the angle limit of thigh motion. Both parameters are known. Through geometric analysis, it is concluded that parameters r_2 and r_3 can represent the geometric structure of hip joint completely. Thus, the main work is to calculate points *E* and *C*. In a reference coordinate system *xyz*, coordinates of points *E* and *C* can be obtained by using vector representation, as shown as equation (1), where trigonometric functions *cosine*() and *sine*() are, respectively, abbreviated as letters *c* and *s*. For example, $\sin(\alpha_d) = s\alpha_d$. Both abbreviated letters *s* and *c* will be used in following equations.

$$\mathbf{r}_C = \begin{bmatrix} x_C \\ y_C \\ z_C \end{bmatrix} = \begin{bmatrix} -r_1\left(s\dfrac{\alpha_d}{4}\right)^2 \\ 0 \\ \dfrac{r_1}{2}\left(s\dfrac{\alpha_d}{2}\right) \end{bmatrix},$$
$$\mathbf{r}_E = \begin{bmatrix} x_E \\ y_E \\ z_E \end{bmatrix} = \begin{bmatrix} -r_1\left(s\dfrac{\alpha_d}{4}\right)^2 \\ 0 \\ \dfrac{r_1}{2}(s\alpha_d) \end{bmatrix}. \quad (1)$$

3.2. Parameterization of Briefs Part. Intuitively, the geometric structure of briefs part is a spherical shell. Neglecting its shell thickness, it consists of three tangent circles, as shown in Figure 6. Those circles correspond to connecting interfaces with waist part, left hip joint, and right hip joint, respectively. Points T_1, T_2, and T_3 are tangent points. Moreover, two global coordinate frames *XYZ* and $X'Y'Z'$ are, respectively, established in the center points of waist part and spherical shell. Left and right circles are designed to have the same inclined angle α_s. Also, a reference coordinate frame *xyz* is established by three points T_1, O_j, and T_3. Angle between coordinate planes *YZ* and *yz* is measured by parameter β_s.

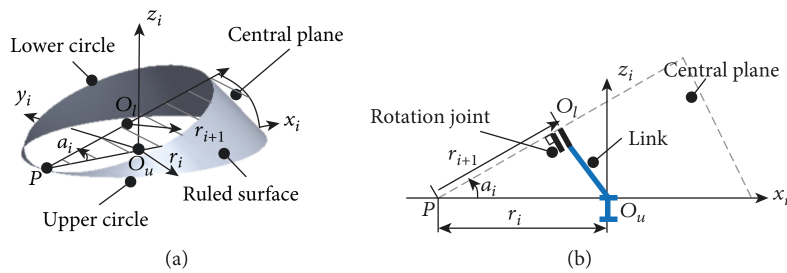

Figure 3: Geometric structure and parameters of (a) joint part and (b) link.

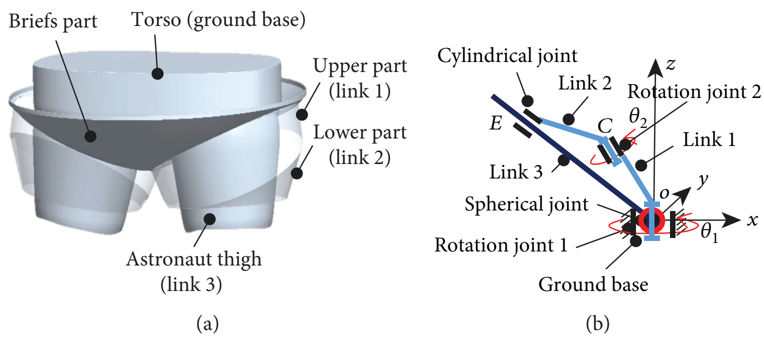

Figure 4: Models of (a) hip joint assembly (b) 3-linkage coupling mechanism.

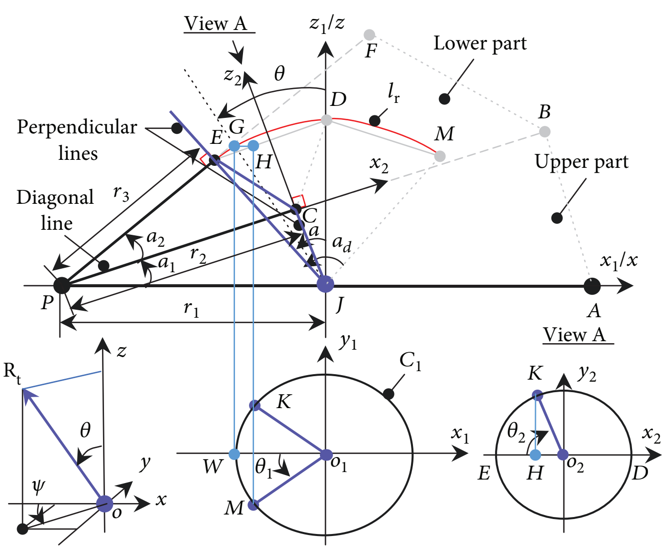

Figure 5: An equiangular dual-perpendicular method.

From Figure 6, it can be seen that structure parameters of briefs part include the radius r_s of spherical shell and two angle parameters α_s and β_s.

Among above three parameters, parameters α_s and α_s are known because they can be determined by design requirements. Therefore, two radiuses r_w and r_s are needed to be calculated, where parameter r_w is the radius of the waist part. From View A-A in Figure 6, radius r_s can be obtained, as shown as

$$r_s = \frac{r_1}{s\alpha_s}. \tag{2}$$

In global coordinate frame $X'Y'Z'$, position vector $\mathbf{R}_S$ of any point S in the left circle of briefs part can be obtained by vector algebra, as shown as

$$\mathbf{R}_S = \begin{bmatrix} \left[\dfrac{r_1 (c\alpha_s)^2}{s\alpha_s} - r_1 s\alpha_s s\gamma\right] s\beta_s - r_1 c\beta_s c\gamma \\ -r_1 c\alpha_s (s\gamma + 1) \\ \left[\dfrac{r_1 (c\alpha_s)^2}{s\alpha_s} - r_1 s\alpha_s s\gamma\right] c\beta_s + r_1 s\beta_s c\gamma \end{bmatrix}, \tag{3}$$

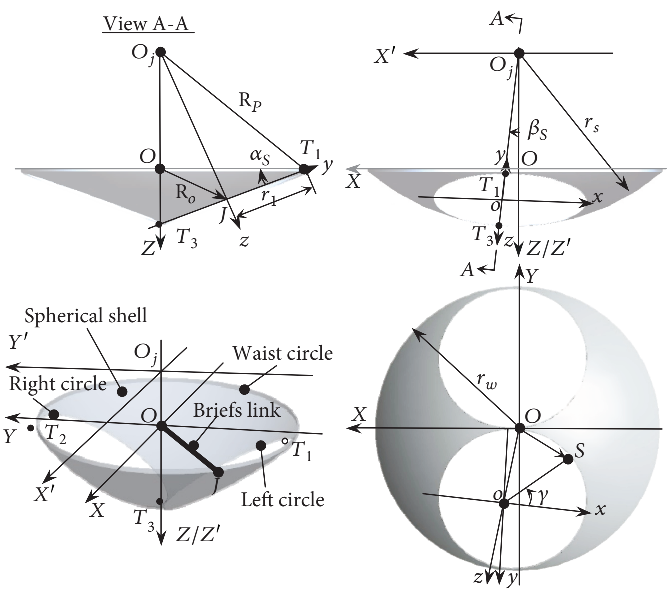

Figure 6: Model and parameters of briefs part.

where parameter γ is the rotation angle of point S about coordinate axis x. According to tangent constraint between waist circle and left circle, angle γ can be obtained by coordinate transformation, as shown as

$$\tan\gamma = -\frac{s\alpha_s c\beta_s}{s\beta_s}. \quad (4)$$

By combining equations (3) and (4), position vector $\mathbf{R}_S$ of any point S in global coordinate frame $X'Y'Z'$ can be rewritten as

$$\mathbf{R}_S = \begin{bmatrix} r_1(c\alpha_s)^2 c\beta_s\left[\dfrac{1}{s\alpha_s} + \sqrt{\dfrac{(c\beta_s)^2}{(s\beta_s)^2+(s\alpha_s c\beta_s)^2}}\right] \\ -r_1 s\alpha_s c\alpha_s\left[\dfrac{1}{s\alpha_s} + \sqrt{\dfrac{(c\beta_s)^2}{(s\beta_s)^2+(s\alpha_s c\beta_s)^2}}\right] \\ r_1 c\beta_s\left[\dfrac{(c\alpha_s)^2}{s\alpha_s} - \sqrt{\left(\dfrac{s\beta_s}{c\beta_s}\right)^2+(s\alpha_s)^2}\right] \end{bmatrix}. \quad (5)$$

Furthermore, radius r_w can be calculated by using coordinates x and y of vector $\mathbf{R}_S$, as shown as

$$r_w = r_1 c\alpha_s\left[\frac{1}{s\alpha_s} + \sqrt{\frac{(c\beta_s)^2}{(s\beta_s)^2+(s\alpha_s c\beta_s)^2}}\right] \times \sqrt{(s\beta_s c\alpha_s)^2+(s\alpha_s)^2}. \quad (6)$$

From equations (1) and (5), it can be seen that parameters of hip joint and briefs part are analytically calculated under the condition of given parameters r_1, α_d, α_s, and β_s. It is known that expressing a vector in different coordinate frame may bring more convenience for calculation. This paper derives translation vector $\mathbf{R}_o$ and transformation matrix $\mathbf{M}_o$ between coordinate frames xyz and XYZ, where parameter $\mathbf{R}_o$ is the position vector of center point J in reference coordinate frame xyz and parameter $\mathbf{M}_o$ is a transformation matrix between coordinate frames xyz and XYZ. Through geometric analysis, both parameters $\mathbf{R}_o$ and $\mathbf{M}_o$ are shown as

$$\mathbf{R}_o = \begin{bmatrix} \dfrac{r_1(c\alpha_s)^2 s\beta_s}{s\alpha_s} \\ -r_1 c\alpha_s \\ r_1\sqrt{(s\beta_s)^2+(s\alpha_s c\beta_s)^2} \end{bmatrix},$$
$$\mathbf{M}_o = \begin{bmatrix} -c\beta_s & 0 & s\beta_s \\ -s\alpha_s s\beta_s & -c\alpha_s & -s\alpha_s c\beta_s \\ c\alpha_s s\beta_s & -s\alpha_s & c\alpha_s c\beta_s \end{bmatrix}. \quad (7)$$

4. Motion Equations of Hip Joint

4.1. Coupling Mechanism Model of Hip Joint Assembly. Firstly, we try to construct the coupling mechanism model of hip joint assembly in global coordinate frame XYZ. In equations (1), (3), and (5), those vectors are derived in reference coordinate frame xyz. However, many gait experiments measure thigh motion in coordinate frame XYZ. To establish motion equation correctly, we must represent hip joint assembly in coordinate frame XYZ. By assembling hip joint with briefs part, a global coupling mechanism model is constructed in coordinate frame XYZ, as shown in Figure 7(b). It looks like a four-linkage mechanism, where briefs part is regarded as a link from origin point O to center point o. Briefs link is fixed in coordinate frame XYZ. To express thigh

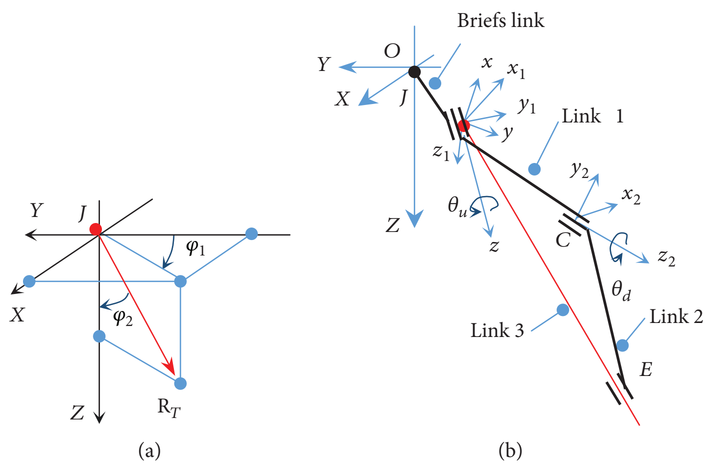

FIGURE 7: Mechanism models of (a) thigh and (b) hip joint assembly.

motion, we define unit vector $\mathbf{R}_T$ to represent link 3 in global coordinate frame XYZ, as shown in Figure 7(a), where link 3 is measured by angle parameters φ_1 and φ_2. Similarly, two parameters θ_d and θ_u represent relative rotation of link 2 and link 1, respectively.

4.2. Motion Equations of Hip Joints. Next, we will derive motion equations of upper part (link 1) and lower part (link 2) in coordinate frame xyz. More details are shown in Figure 5, where unit vector $\mathbf{R}_t$ is illustrated to represent segment line JE. Obviously, it can be measured by two parameters θ and ψ. For a given angle θ, segment line JE moves to segment line JG. From point G, a parallel line GH is drawn to intersect line ED at point H. Point W is the projection of point G in coordinate plane x_1y_1. Then, circle C_1 is formed through point W. From point H, vertical line HM intersects with circle C_1 at points K and M. It is concluded that rotation of upper part can be measured by parameter $\theta_1 = \angle WoM$. In View A, motion trajectory of lower part can be expressed by circle C_2. Then, vertical line HK is drawn to intersect with circle C_2 at point K. Relative rotation of lower part can be calculated by parameter $\theta_2 = \angle Ho_2K$.

From circle C_1, it can be seen that length l_k of line Ko_1 equals to length l_w of line Wo_1. In coordinate frame xyz, coordinates of points K and G can be obtained in a form of vectors $\mathbf{R}_K$ and $\mathbf{R}_G$, as shown as

$$\mathbf{R}_K = \begin{bmatrix} -\dfrac{r_1\left(s(\alpha_d/2)\right)^2}{2}\left(c\theta_2 + 1\right) \\ r_1 s\dfrac{\alpha_d}{2} s\dfrac{\alpha_d}{4} s\theta_2 \\ -r_1 s\dfrac{\alpha_d}{2}\left[\left(s\dfrac{\alpha_d}{4}\right)^2 c\theta_2 + \left(c\dfrac{\alpha_d}{4}\right)^2\right] \end{bmatrix}, \qquad (8)$$

$$\mathbf{R}_G = \begin{bmatrix} -r_1 s\dfrac{\alpha_d}{2} s\theta \\ 0 \\ r_1 s\dfrac{\alpha_d}{2} c\theta \end{bmatrix}.$$

Because of $l_k = l_w$, parameters θ_1 and θ_2 can be derived, as shown as

$$\begin{cases} s\theta_1 = \dfrac{1}{s(\alpha_d/4)}\sqrt{\dfrac{c\theta - c(\alpha_d/2)}{1 + c\theta}}, \\ c\theta_2 = \dfrac{\left(c(\alpha_d/4)\right)^2 - c\theta}{\left(s(\alpha_d/4)\right)^2}, \end{cases} \quad \theta \in \left[-\frac{\alpha_d}{2} \quad 0\right),$$

$$\begin{cases} s\theta_1 = \pi - \dfrac{1}{s(\alpha_d/4)}\sqrt{\dfrac{c\theta - c(\alpha_d/2)}{1 + c\theta}}, \\ c\theta_2 = 2\pi - \dfrac{1 + \left(c(\alpha_d/4)\right)^2 c\theta}{\left(s(\alpha_d/4)\right)^2}, \end{cases} \quad \theta \in \left[0 \quad \frac{\alpha_d}{2}\right]. \qquad (9)$$

Secondly, we will derive thigh motion equation in coordinate frame xyz. In Figure 7, unit vector $\mathbf{R}_T$ can be written as equation (10) in coordinate frame XYZ.

$$\mathbf{R}_T = \begin{bmatrix} s\varphi_2 s\varphi_1 \\ -s\varphi_2 c\varphi_1 \\ c\varphi_2 \end{bmatrix}. \qquad (10)$$

By coordinate transformation, unit vector $\mathbf{R}_T$ can be expressed as vector $\mathbf{R}_t$ in coordinate frame xyz, as shown as

$$\mathbf{R}_t = \mathbf{M}_o \mathbf{R}_T. \qquad (11)$$

By substituting equations (7) and (10) into equation (11), vector $\mathbf{R}_t$ can be rewritten as

$$\mathbf{R}_t = \begin{bmatrix} s\beta_s c\varphi_2 - c\beta_s s\varphi_1 s\varphi_2 \\ \left(c\alpha_s c\varphi_1 - s\alpha_s s\beta_s s\varphi_1\right)s\varphi_2 - s\alpha_s c\beta_s c\varphi_2 \\ \left(s\alpha_s c\varphi_1 + c\alpha_s s\beta_s s\varphi_1\right)s\varphi_2 + c\alpha_s c\beta_s c\varphi_2 \end{bmatrix}. \qquad (12)$$

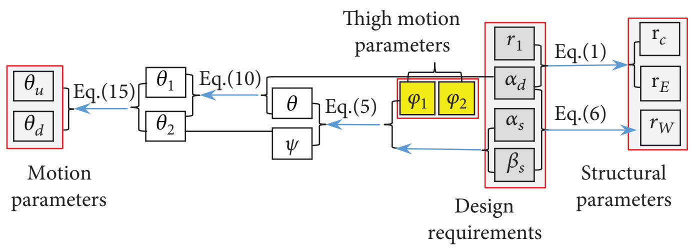

Figure 8: Computation procedure.

From Figure 5, it can be seen that vector $\mathbf{R}_T$ can also be written as vector $\mathbf{R}_{ts}$ in a form of parameters θ and ψ.

$$\mathbf{R}_{ts} = \begin{bmatrix} -s\theta c\psi \\ -s\theta s\psi \\ c\theta \end{bmatrix}. \tag{13}$$

According to $\mathbf{R}_t = \mathbf{R}_{ts}$, parameters θ and ψ can be calculated by

$$\begin{cases} \tan\psi = \dfrac{(c\alpha_s c\varphi_1 - s\alpha_s s\beta_s s\varphi_1)s\varphi_2 - s\alpha_s c\beta_s c\varphi_2}{s\beta_s c\varphi_2 - c\beta_s s\varphi_1 s\varphi_2}, \\ \cos\theta = (c\alpha_s s\beta_s s\varphi_1 + s\alpha_s c\varphi_1)s\varphi_2 + c\alpha_s c\beta_s c\varphi_2. \end{cases} \tag{14}$$

Based on the relationship between planar rotation and fixed axis rotation, parameters θ_d and θ_u can be derived in coordinate frame XYZ, as shown as

$$\begin{cases} \theta_u = \theta_1 + \psi, \\ \theta_d = \theta_2. \end{cases} \tag{15}$$

Above all, motion equations (equation (15)) of lower part and upper part have been established analytically. Of course, thigh status (θ, ψ) can be calculated under condition of given ration angles (θ_d, θ_u) of hip joint.

For convenience of programming, computation procedure is given to solve design parameters and motion equations based on known conditions, as shown in Figure 8, where parameters r_1, α_{d}, α_s, and β_s are known as mentioned before. Parameters $\mathbf{r}_c$, $\mathbf{r}_E$, and r_w, respectively, represent the geometric structure of hip joint parts and briefs part. Parameters θ_u and θ_d are the rotation angle of upper part and lower part. Parameters φ_1 and φ_2 express thigh motion, which are input for equation (15). Firstly, we determine parameters r_1, α_d, α_s, and β_s according to design requirement. Then, using equations (10) and (15) solve hip joint motion for any given thigh parameters. Finally, structural parameters are calculated by equations (1) and (6).

4.3. A Case Study. Based on above computation procedure, related program was developed to carry out a case study, where design parameters are set to $r_1 = 113\,\mathrm{mm}$, $\alpha_d = 80^\circ$, $\alpha_s = 20^\circ$, and $\beta_s = 5^\circ$. Thigh data had been downloaded from the website [21]. Only flexion/extension data are adopted.

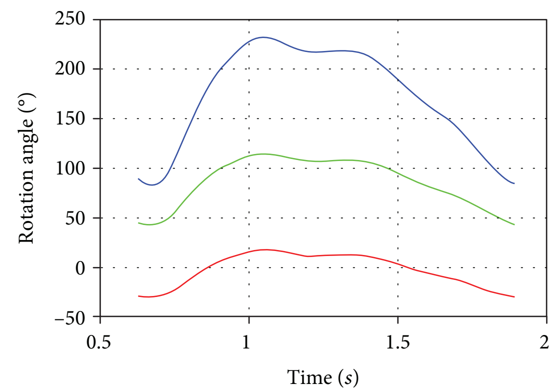

Figure 9: Motion curves of upper part (green solid curve) and lower part (blue solid curve) and thigh (red solid curve).

According to above computation procedure, motion equations of hip joint can be computed and plotted in Figure 9. It can be seen that both curves of parameters θ_u and θ_d are smooth and continuous. They are consistent with theoretical expect. Above all, our proposed representation method and coupling model are correct and feasible.

5. Conclusion

Around a coupling effect of hip joint and thigh, this paper proposes an equiangular dual-perpendicular method to design a conceptual model of hip joint. Geometric structure and coupling constraints are discussed in detail. Specifically speaking, two perpendicular constraints are given out to avoid impact between hip joint and thigh. Symmetric and coincident constraints are brought out to realize thigh continuous motion. Based on above constraints, a 3-linkage coupling mechanism model is built up. Motion equations of hip joint are derived by using coordinate transformation and vector representation. Meanwhile, related computation procedure is formed to solve structural parameters and motion parameters, respectively. Finally, a case study is conducted to verify the proposed representation method and motion equations. Results show that the conceptual design of hip joint is correct and feasible.

Data Availability

No data were used to support this study.

Conflicts of Interest

The authors declare that they have no conflicts of interest.

Acknowledgments

The National Natural Science Foundation of China under the grant No. 51675087 supports this research.

References

[1] A. P. Anderson and D. J. Newman, "Pressure sensing for in-suit measurement of space suited biomechanics," *Acta Astronautica*, vol. 115, pp. 218–225, 2015.

[2] B. Holschuh, J. Waldie, J. Hoffman, and D. Newman, "Characterization of structural, volume, and pressure components to space suit joint rigidity," in *Proceeding of the International Conference on Environmental Systems, Society of Automotive Engineers*, Savannah, GA, USA, 2009.

[3] S. M. McFarland, "Z-2 space suit: a case study in human spaceflight public outreach," in *46th International conference on Environmental Systems*, pp. 10–14, Vienna, Austria, July 2016.

[4] A. Anderson, A. Hilbert, and P. Bertrand, "In-suit sensor systems for characterizing human-space suit interaction," in *44th International Conference on Environmental Systems*, pp. 13–17, Tucson, AZ, USA, July 2014.

[5] C. R. Cullinane, R. A. Rhodes, and L. A. Stirling, "Mobility and agility during locomotion in the Mark III space suit," *Aerospace Medicine and Human Performance*, vol. 88, no. 6, pp. 589–596, 2017.

[6] P. J. Bertrand, A. Anderson, A. Hilbert, and D. Newman, "Feasibility of spacesuit kinematics and human-suit interactions," in *44th international conference on environmental systems*, pp. 23–27, Tucson, AZ, USA, July 2014.

[7] J. Hochstein, *Astronaut total injury database and finger/hand injuries during EVA training and tasks*, International Space University, Strasbourg, France, 2008.

[8] P. Schmidt, *An investigation of space suit mobility with applications to EVA operations, [Ph.D. thesis]*, Massachusetts Institute of Technology, Cambridge, MA, USA, 2001.

[9] M. G. C. Lewis, M. R. Yeadon, and M. A. King, "The effect of accounting for biarticularity in hip flexor and hip extensor joint torque representations," *Human Movement Science*, vol. 57, pp. 388–399, 2018.

[10] M. S. Cowley, E. J. Boyko, J. B. Shofer, J. H. Ahroni, and W. R. Ledoux, "Foot ulcer risk and location in relation to prospective clinical assessment of foot shape and mobility among persons with diabetes," *Diabetes Research and Clinical Practice*, vol. 82, no. 2, pp. 226–232, 2008.

[11] M. Wehner, B. Quinlivan, P. M. Aubin et al., "A lightweight soft exosuit for gait assistance," in *2013 IEEE International Conference on Robotics and Automation*, pp. 3362–3369, Karlsruhe, Germany, 2013.

[12] P. M. Aubin, M. S. Cowley, and W. R. Ledoux, "Gait simulation via a 6-DOF parallel robot with iterative learning control," *IEEE Transactions on Biomedical Engineering*, vol. 55, no. 3, pp. 1237–1240, 2008.

[13] L. T. Aitchision, "A comparison of methods for assessing space suit joint ranges of motion," in *42nd International Conference on Environmental Systems*, p. 3534, San Diego, CA, USA, 2012.

[14] T. McGrath, R. Fineman, and L. Stirling, "An auto-calibrating knee flexion-extension axis estimator using principal component analysis with inertial sensors," *Sensors*, vol. 18, no. 6, p. 1882, 2018.

[15] L. Stirling, K. Willcox, and D. Newman, "Development of a computational model for astronaut reorientation," *Journal of Biomechanics*, vol. 43, no. 12, pp. 2309–2314, 2010.

[16] C. R. Cullinane, *Evaluation of the Mark III spacesuit-an experimental and computational modeling approach*, Massachusetts Institute of Technology, 2018.

[17] L. Stirling, H. C. Siu, E. Jones, and K. Duda, "Human factors considerations for enabling functional use of exosystems in operational environments," *IEEE Systems Journal*, vol. 13, no. 1, pp. 1072–1083, 2019.

[18] R. A. Fineman, T. M. McGrath, D. G. Kelty-Stephen, A. F. J. Abercromby, and L. A. Stirling, "Objective metrics quantifying fit and performance in spacesuit assemblies," *Aerospace Medicine and Human Performance*, vol. 89, no. 11, pp. 985–995, 2018.

[19] D. Graziosi, B. Jones, J. Ferl, S. Scarborough, and L. Hewes, "Z-2 architecture description and requirements verification results," in *46th International Conference on Environmental Systems*, pp. 10–14, Vienna, Austria, July, 2016.

[20] M. S. Cowley, S. Margerum, L. Harvill, and S. Rajulu, "Chapter XX: model for predicting the performance of planetary suit hip bearing designs," https://ntrs.nasa.gov/search.jsp?R=20130000596.

[21] http://www.cbsr.ia.ac.cn/users/szheng/?page_id=389.